RESEARCH ARTICLE

GROUNDWATER

Predictions of groundwater PFAS occurrence at drinking water supply depths in the United States

Andrea K. Tokranov[1]*, Katherine M. Ransom[2]†, Laura M. Bexfield[3], Bruce D. Lindsey[4], Elise Watson[5], Danielle I. Dupuy[2], Paul E. Stackelberg[6], Miranda S. Fram[2], Stefan A. Voss[2], James A. Kingsbury[7], Bryant C. Jurgens[2], Kelly L. Smalling[8], Paul M. Bradley[9]

Per- and polyfluoroalkyl substances (PFAS), known colloquially as "forever chemicals," have been associated with adverse human health effects and have contaminated drinking water supplies across the United States owing to their long-term and widespread use. People in the United States may unknowingly be drinking water that contains PFAS because of a lack of systematic analysis, particularly in domestic water supplies. We present an extreme gradient–boosting model for predicting the occurrence of PFAS in groundwater at the depths of drinking water supply for the conterminous United States. Our model results indicate that 71 million to 95 million people in the conterminous United States potentially rely on groundwater with detectable concentrations of PFAS for their drinking water supplies before any treatment.

Per- and polyfluoroalkyl substances (PFAS) are synthetic, highly persistent contaminants with global prevalence in many environmental matrices (*1*). Several adverse human and ecosystem effects have been linked to exposure (*2*–*4*), driving international public concern and prompting guidelines and regulations for drinking water (*1*, *5*, *6*). In the United States, substantial resources have been dedicated to monitoring drinking water supplies (*7*–*9*). The US Environmental Protection Agency (EPA) fifth Unregulated Contaminant Monitoring Rule (UCMR 5) requires monitoring for 29 PFAS between 2023 and 2025 with the goal of sampling all public water systems that serve more than 3300 people and 800 representative small public water supplies that serve less than 3300 people (*9*). However, the UCMR 5 sampling does not include over 90% of small public water supplies that serve less than 3300 people (*10*) or domestic well users (those with private household wells) that account for ~13% of the population in the United States (*11*). Additionally, precise locations and well depths of UCMR 5 samples are not disclosed to protect drinking water security. These data limitations may hinder effective water management decisions. To address such gaps, recent studies have developed statewide models to predict PFAS concentrations and occurrence (*12*–*15*). PFAS analysis is expensive and time intensive, precluding the monitoring of every household's drinking water. Models that predict PFAS occurrence can direct limited resources to areas identified as having a high likelihood of occurrence (*16*).

We present a national predictive model of PFAS occurrence in groundwater at the depths of drinking water supplies across the conterminous United States, before any treatment. We trained the model on groundwater samples collected by the US Geological Survey (USGS) since 2019 (table S1, USGS data release) (*17*) using eXtreme Gradient Boosting (XGBoost) (*18*), an ensemble tree method. An estimated 140 million people (over 40% of the population) in the United States rely on groundwater as a source of drinking water (*19*, *20*). We hypothesized that a robust model to predict PFAS occurrence in groundwater could be built on mappable factors, obviating the need for an impractical approach of using well-specific chemistry as predictor variables. The purpose was to predict PFAS occurrence in unmonitored locations to help identify areas that may be a priority for future monitoring.

We collected PFAS samples between 2019 and 2022 in three types of well networks within principal aquifers (*21*, *22*); principal aquifers are large aquifer systems that collectively account for the majority of the nation's groundwater usage (*22*–*25*). The three types of well networks are (i) public supply networks spanning principal aquifers (*22*), (ii) observation networks targeting urban and agricultural land uses (*26*), and (iii) domestic supply well networks in principal aquifers (*26*). The network names, network types, and associated principal aquifers can be found in table S1 and figs. S1 to S3. All networks were strategically designed by using an equal-area grid approach to reflect groundwater quality within each network (*21*–*24*). Samples have known well depths, were collected with consistent sampling protocols before any water treatment, and were analyzed at the same laboratory to ensure quality (tables S2 to S4) (*27*).

Relationships between groundwater PFAS data and explanatory variables identified by our model in sampled principal aquifers were used to predict groundwater PFAS occurrence nationally. We conducted extensive PFAS source mapping (table S5 and fig. S4), and our final model included 25 potential PFAS sources such as airports, metal coating facilities, plastics and resins facilities, printing facilities, fire training areas, chemical manufacturing facilities, and national defense sites, among many others. We grouped these variables into a single parameter to simplify the model after iterative model runs indicated little difference between splitting and grouping these potential PFAS source variables. We included nitrogen loading from septic systems as a proxy for septic system releases (*28*). An advantage of XGBoost is that it can handle interactions between variables (*29*–*31*). XGBoost can also handle missing data and outliers and does not require prior data transformation (*29*). However, highly correlated variables (absolute Pearson's correlation coefficient >0.6) were removed during model development because they did not improve model performance. Information on well networks, quality control data, model structure, and model inputs are available in (*27*) (figs. S1 to S8 and tables S1 to S5).

We converted the sum of 24 individual PFAS in the training data to a binary variable (detected or not detected) to model occurrence of any PFAS compound. This approach was chosen because (i) PFAS are commonly found in mixtures in the environment (*3*, *7*), (ii) there are rising concerns over human-health effects from exposure to several different PFAS (*3*), and (iii) drinking water guidelines and regulations over the past decade have called for much lower allowable levels of PFAS in drinking water to be protective of human health; currently, a maximum contaminant level (MCL) of 4 ng/liter is set by the EPA for perfluorooctane sulfonate (PFOS) and perfluorooctanoate (PFOA) (*5*, *6*). The most common method detection limit (MDL) across the training dataset ranged between 1 and 1.9 ng/liter depending on the compound (*27*), which is between the maximum contaminant level goal (MCLG) of 0 ng/liter and the MCL (4 ng/liter) for PFOS and PFOA and within the documented range for health effects (*6*, *32*).

Results and discussion

High rates of occurrence of PFAS in model training data

At least one PFAS out of the 24 individual PFAS analyzed was detected in 37% (n = 1238) of the groundwater samples analyzed for the model training dataset (Fig. 1 and table S1). MDLs

[1]US Geological Survey, Pembroke, NH 03275, USA. [2]US Geological Survey, Sacramento, CA 95819, USA. [3]US Geological Survey, Albuquerque, NM 87113, USA. [4]US Geological Survey, New Cumberland, PA 17070, USA. [5]US Geological Survey, San Diego, CA 92101, USA. [6]US Geological Survey, Troy, NY 12180, USA. [7]US Geological Survey, Nashville, TN 37211, USA. [8]US Geological Survey, Lawrenceville, NJ 08648, USA. [9]US Geological Survey, Columbia, SC 29210, USA.
*Corresponding author. Email: atokranov@usgs.gov
†Present address: ORCaS, San Rafael, CA 94901, USA.

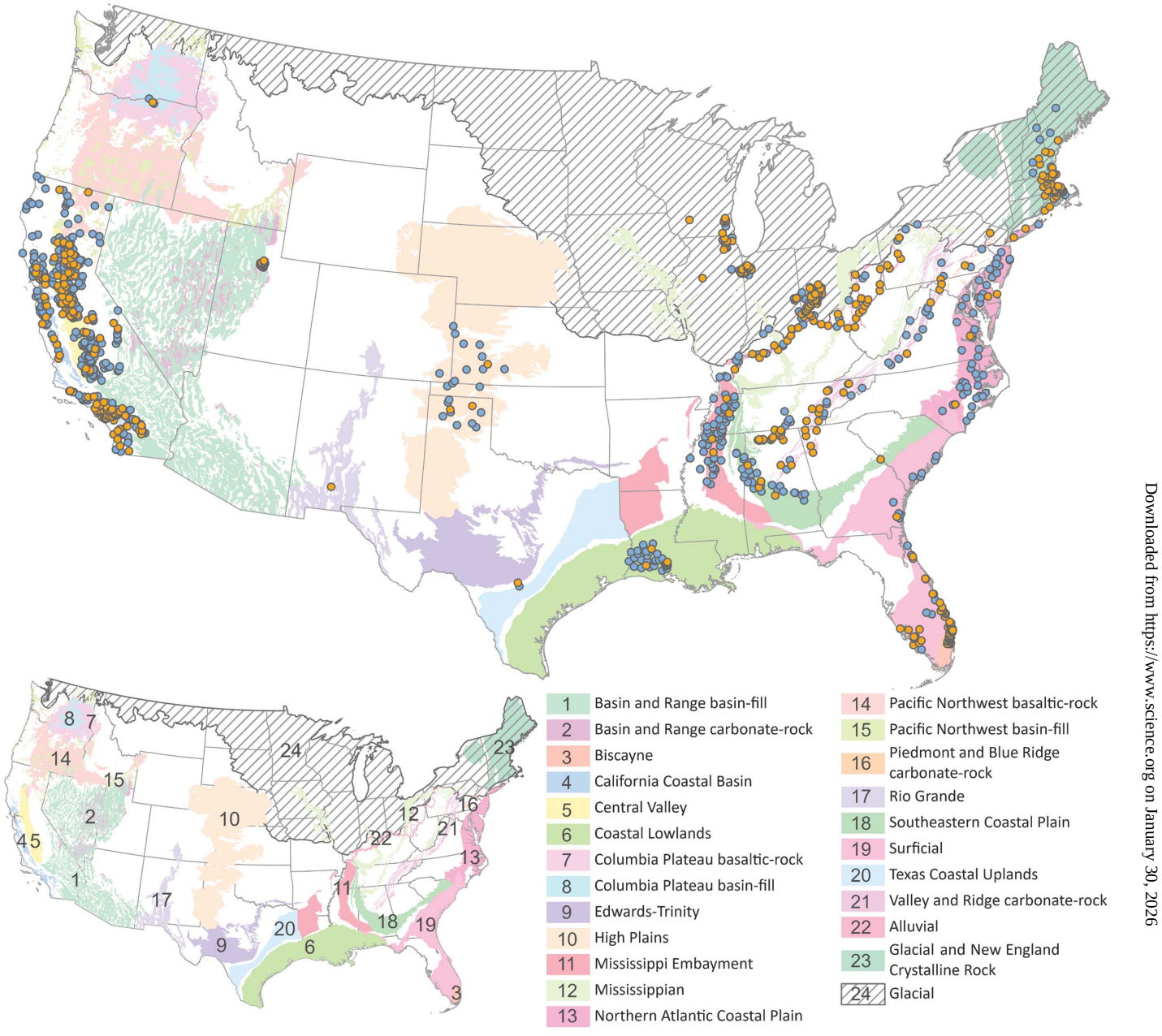

Fig. 1. Principal aquifers of the United States and groundwater sample locations analyzed for PFAS. Principal aquifers of the United States (*25*) are overlain by PFAS sampling locations (circles) used for model training. Orange circles indicate PFAS detected; blue circles indicate PFAS not detected.

changed by analysis date and compound but did not vary substantially [(*27*), Method detection limits] (*17*). Observation wells had the highest occurrence rate (detection frequency) of any PFAS at 60% (n = 257), followed by production (public supply) wells (42%, n = 539); miscellaneous, other, and irrigation wells (29%, n = 59); and domestic wells (17%, n = 383). The higher detection frequencies found for observation wells may be because the wells are typically shallower than other well types (fig. S1B) because they were designed to monitor shallow water in agricultural and urban land use settings (*26*). By individual compound, the highest detection frequencies were observed for perfluorobutane sulfonate (PFBS; 24.6%), PFOS (24.3%), PFOA (24.1%), and perfluorohexane sulfonate (PFHxS; 23.7%). All four compounds are included in the EPA's PFAS National Primary Drinking Water Regulation rulemaking (*6*). Total PFAS concentrations varied by aquifer and well network (figs. S1 and S2), with the highest median concentration of 29 ng/liter for the sum of 24 PFAS occurring in the Biscayne Principal Aquifer in southern Florida (Fig. 1 and fig. S1). These detection frequencies are commensurate with other work that estimates 38% of groundwater in the United States is modern in age (recharged since 1953) (*33*). Holocene groundwater (~75 to 11,800 years ago) may be expected to have some PFAS detections for the most recent fraction, whereas PFAS detections are not expected in Pleistocene-age groundwater recharged >11,800 years ago.

Model characteristics

The XGBoost model selected from 10-fold cross-validation tuning was composed of 250 trees, an interaction depth of 3, learning rate of 0.0505,

Table 1. Detection frequency, accuracy, specificity, and sensitivity results from evaluation of independent datasets against model predictions by using thresholds of 0.315 and 0.5.

	Observed detection frequency (*n*)	Modeled detection frequency (*n*)	Model threshold	Accuracy (*n*)	Specificity (*n*)	Sensitivity (*n*)
UCMR 5*	0.27 (2633)	0.41 (2633)	0.315	0.64 (2633)	0.66 (1915)	0.59 (718)
UCMR 5		0.26 (2633)	0.5	0.67 (2633)	0.78 (1915)	0.37 (718)
UCMR 5, states without model training data*	0.16 (639)	0.35 (639)	0.315	0.68 (639)	0.70 (538)	0.60 (101)
UCMR 5, states without model training data*		0.24 (639)	0.5	0.75 (639)	0.80 (538)	0.46 (101)
UCMR 5, states with model training data*	0.31 (1985)	0.43 (1985)	0.315	0.63 (1985)	0.64 (1373)	0.59 (612)
UCMR 5, states with model training data*		0.26 (1985)	0.5	0.65 (1985)	0.78 (1373)	0.36 (612)
USGS domestic tapwater	0.22 (255)	0.40 (255)	0.315	0.62 (255)	0.64 (200)	0.56 (55)
USGS domestic tapwater		0.26 (255)	0.5	0.73 (255)	0.80 (200)	0.47 (55)
USGS domestic tapwater, states without model training data	0.12 (129)	0.21 (129)	0.315	0.71 (129)	0.79 (113)	0.19 (16)
USGS domestic tapwater, states without model training data		0.12 (129)	0.5	0.78 (129)	0.88 (113)	0.13 (16)
USGS domestic tapwater, states with model training data	0.31 (126)	0.60 (126)	0.315	0.53 (126)	0.45 (87)	0.72 (39)
USGS domestic tapwater, states with model training data		0.40 (126)	0.5	0.67 (126)	0.69 (87)	0.62 (39)
Wisconsin domestic well water	0.32 (448)	0.26 (448)	0.315	0.63 (448)	0.78 (303)	0.34 (145)
Wisconsin domestic well water		0.1 (448)	0.5	0.67 (448)	0.92 (303)	0.16 (145)
Wisconsin domestic well water, <40 feet below water table	0.35 (40)	0.25 (40)	0.315	0.70 (40)	0.85 (26)	0.43 (14)
Wisconsin domestic well water, <40 feet below water table		0.15 (40)	0.5	0.75 (40)	0.96 (26)	0.36 (14)
Wisconsin public supply	0.17 (1537)	0.41 (1537)	0.315	0.64 (1537)	0.63 (1275)	0.64 (262)
Wisconsin public supply		0.23 (1537)	0.5	0.74 (1537)	0.81 (1275)	0.42 (262)

*Assuming a median threshold where 50% of the cells within the ZIP codes reporting UCMR 5 results were required to be predicted as a detection to count the ZIP code block as a detection.

and loss reduction of 0.1. The output of the model is a probability of PFAS detection for each grid cell (each 1 by 1 km in size) across the conterminous United States. Various thresholds can be selected, above which a PFAS detection was predicted. For example, if a threshold of 0.5 is chosen, then any grid cell with a probability value greater than 0.5 is an area where PFAS is predicted to occur. Threshold tuning indicated a probability cutoff of 0.315 optimized model performance and provided a reasonable balance between sensitivity and specificity. Sensitivity is the fraction of correctly predicted detections, and specificity is the fraction of correctly predicted nondetects. Accuracy is the overall fraction of correct predictions (nondetects and detects combined). A threshold of 0.5 is standard model practice (*31*, *34*) and provides a conservative estimate of PFAS detections. We evaluated both the 0.5 and 0.315 thresholds. Implementing a standard threshold of 0.5, the accuracy of the model was 0.78 (standard error, 0.0098), the sensitivity was 0.63 (0.0155), and the specificity was 0.86 (0.0198). The receiver operator characteristics (ROC) curve plots the true positive rate over the false positive rate (1 – specificity), and the area under the curve provides a metric of model performance, with 1 being the maximum. This model produced an ROC of 0.83, which is classified as a "good" model (*35*). When using the threshold-tuned cutoff of 0.315, the overall accuracy of the model was 0.77 (0.0098), the sensitivity was 0.79 (0.0164), and the specificity was 0.75 (0.0203). ROC does not change dependent on threshold. These model metrics are comparable with our previous work in the eastern United States in which the accuracy, sensitivity, and specificity for holdout data were 0.84, 0.96, and 0.72, respectively (*7*). Modeled versus observed detection frequencies for each well network indicated good agreement, with coefficient of determination (R^2) values of 0.70 for public supply and 0.51 for domestic supply networks, using a threshold of 0.315 (fig. S9).

Model estimates of PFAS in groundwater

Model results (Fig. 2) indicate widespread occurrence of PFAS in groundwater at depths of public and domestic drinking water supplies (*36*). The depths of public and domestic drinking water supplies vary by grid cell and reflect the moving median surface of the depth to the bottom of the groundwater withdrawal zone (fig. S10) (*36*). Depending on the probability threshold for classifying a detection (presented as the results for a threshold of 0.5 followed by the results for a threshold of 0.315 in parentheses), the groundwater area predicted to be affected is 430,000 km^2 (980,000 km^2) at the depth of public water supply and 560,000 km^2 (1,200,000 km^2) at the depth of domestic supply. These account for ~5.5% (13%) (public) and 7.2% (15%) (domestic) of the area of the conterminous

United States. The results (particularly the results for a threshold of 0.315) align well with recent data that indicate a 20% detection frequency in domestic well tap water (*8*) and an 18% detection frequency for distinct public water systems with groundwater identified as the source water in the first batch of UCMR 5 data released in July 2023 (*37*).

We estimated the population that is reliant on groundwater with detectable concentrations of PFAS for each grid cell by summing the estimated population of domestic well users (*20*) and the equivalent population reliant on groundwater-based public water supply (*19*) within each grid cell (tables S6 to S8). For public supply, we calculated the equivalent population as the public supply groundwater fraction (the fraction of public supply sourced from groundwater) multiplied by the total population that uses public supply (*19*). We calculated population estimates three ways. The first two methods used the two thresholds (0.315 and 0.5) to predict whether a grid cell contained detectable PFAS. For example, if a grid cell exceeded the given threshold, then 100% of the population reliant on groundwater was assumed to be affected. The third method used the raw probability for each grid cell (no threshold applied) multiplied by the estimated population reliant on groundwater for that grid cell. The model standard error from 10-fold cross-validation was carried through to population estimates and used to compute 95% confidence intervals (CIs) for all three methods. Using these methods, a total of 71 million (95 CI: 70 million, 73 million) to 95 million (CI: 93 million, 97 million) people are estimated to source their drinking water from groundwater with detectable concentrations of PFAS (table S8). Of these total estimates, equivalent public supply accounts for 58 million (CI: 57 million, 59 million) to 77 million (CI: 76 million, 79 million) people, and domestic supply accounts for 11 million (CI: 11 million, 12 million) to 18 million (CI: 18 million,18 million) people (tables S6 and S7). This represents 50% (CI: 49%, 51%) to 66% (CI: 65%, 66%) of the total population that is drinking water from public or domestic supply with water sourced from groundwater. For public supply groundwater, Florida and California had the highest equivalent populations estimated to be affected [9.5 million (CI: 9.3 million, 9.7 million) to 13 million (CI: 13 million, 13 million) people], whereas Massachusetts had the highest percentage of equivalent population predicted to be affected for public supply [86% (CI: 84%, 88%) to 98% (CI: 96%, 99%)]. For domestic supply, Michigan and Florida had the highest populations estimated to be affected by groundwater with detectable concentrations of PFAS [Michigan, 0.92 million (CI: 0.90 million, 0.94 million) to 1.4 million (CI: 1.4 million, 1.4 million) people; Florida, 0.99 million (CI: 0.97 million, 1.0 million) to 1.3 million (CI: 1.3 million, 1.3 million) people]. The District of Columbia had the highest percentage of population that uses domestic supply predicted to be affected by PFAS [76% (CI: 74%, 77%) to 95% (CI: 93%, 97%)], but the total population that uses domestic supply is very low (estimated ~500 people). These estimates are dependent on several factors, including location of drinking water intakes and drinking water treatment. The model predicts groundwater occurrence, so all estimates are for untreated groundwater. Many public water suppliers have recently started to monitor and treat for PFAS, and therefore, these public-supply predictions may be overestimates because water utilities actively seek PFAS-free water intakes and implement remediation solutions. However, removing PFAS from drinking water is expensive and can be particularly cost prohibitive for low-income communities, which has impeded progress toward clean drinking water supplies (*38*). Domestic well owners often do not test or treat their water (*39*, *40*) and may therefore be more susceptible to local groundwater PFAS contamination. The proportion of the population predicted to have drinking water sourced from groundwater with detectable

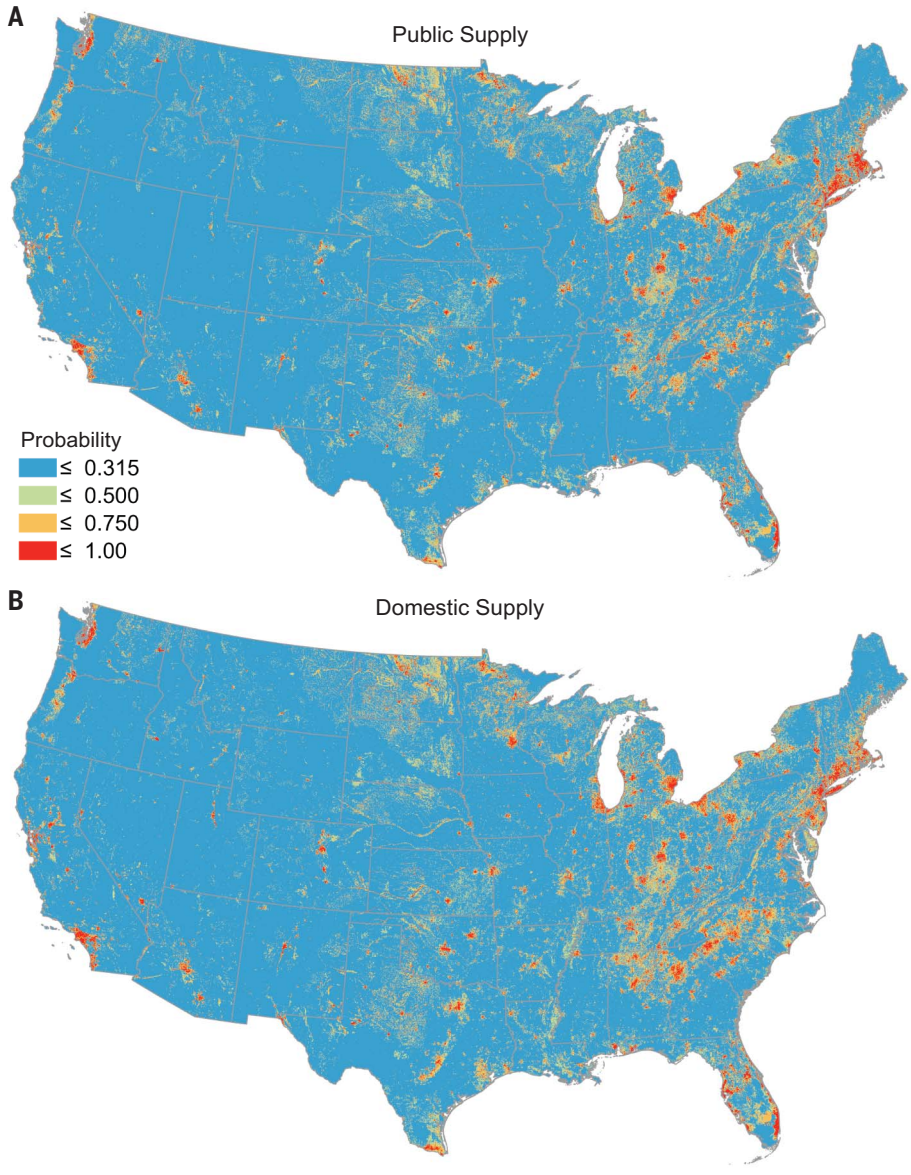

Fig. 2. Probability of PFAS occurrence in groundwater. (**A** and **B**) Probability of PFAS occurrence in groundwater before any treatment at the depths of the bottom of (A) public drinking water supplies and (B) domestic drinking water supplies. Depths used for prediction vary by grid cell across the conterminous United States.

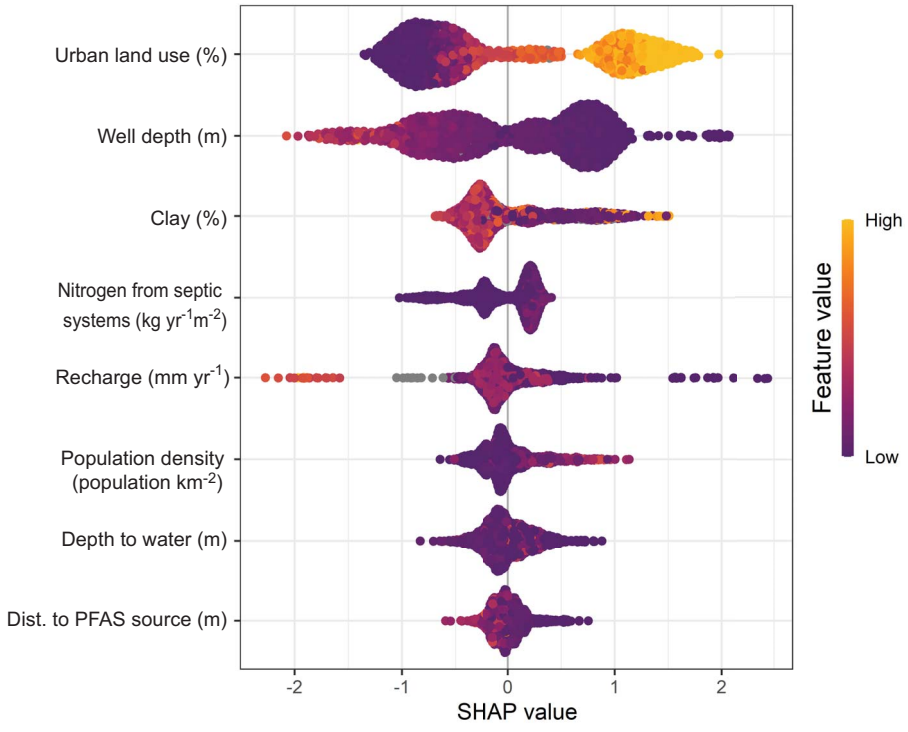

Fig. 3. SHAP plot for model training data for detection of PFAS. Variables are organized from most to least important (fig. S11) from top to bottom of the figure. Positive SHAP values correspond to an increased probability of detection and vice versa (SHAP value units are in log odds). SHAP values are computed relative to the average prediction, indicated as zero on the *x* axis. Colors on the SHAP plot range from low (purple) to high (yellow) values of the predictor variable. Missing values are shown in gray.

concentrations of PFAS is disproportionally large compared with the area of land affected because areas with high population and greater urban density are also more likely to be affected by PFAS contamination.

Variable importance and relationships to predictions

Model variable importance in order of decreasing importance for the training dataset was (i) percent of urban land use; (ii) well depth; (iii) percent clay in soil; (iv) estimated nitrogen loading from septic systems; (v) average annual natural groundwater recharge (excludes irrigation and imported water); (vi) population density; (vii) depth to groundwater; and (viii) distance to the nearest site potentially containing, using, or emitting PFAS (Fig. 3 and fig. S11). Our model predictions across the conterminous United States resulted in a similar order of model variable importance compared with the training data (fig. S12). We used SHAP values [SHapley Additive exPlanations (*41*)] to help interpret model results by assigning values for the contribution of each variable to individual predictions (*30*, *41*). High values of urban land use had positive SHAP values, indicating a greater likelihood of predicted PFAS occurrence. The percentage of urban land use was also identified as one of the top predictor variables in our previous modeling work (*7*, *8*). Similarly, higher population densities resulted in positive SHAP values. Both urban land use and population density trends likely reflect the multitude of PFAS sources expected to exist in populated areas (*42*). Links between population density and PFAS in soil were previously demonstrated in Tianjin, China (*43*); Sweden (*44*); and Vermont (*45*). Although urban land use and population density are correlated (fig. S13), the model has identified urban land use as the best variable for model variance reduction. However, both variables are important to the model, indicating that population density provides additional information to the model that further reduces variance. This is also the case for other correlated variables in the final model (fig. S13).

Shallow well depths and shallow depths to water also had positive SHAP values. Groundwater depth is generally correlated with groundwater age, with shallow well depths more likely to be reflective of recent recharge (*7*, *46*). PFAS are anthropogenic compounds first developed in the 1930s and therefore are only expected to be present in groundwater that includes modern recharge. Groundwater used for drinking water supplies in the United States ranges from modern to Pleistocene (>11,800 years) in age (*33*). PFAS have been detected in rainfall and in soils globally with no known local point sources (*1*), suggesting that there are anthropogenic background concentrations of PFAS and that recent recharge may result in PFAS detections (*7*). Global occurrence of PFAS may explain the trends seen with natural recharge (which does not include irrigation or imported water), in which very low values of recharge were associated with positive SHAP values and very high values of recharge were associated with negative SHAP values. Aside from the extreme values of recharge at the low and high end, the majority of the SHAP values hover around zero, indicating a complicated relationship. High values of natural recharge may result in dilution of PFAS concentrations to levels below detection limits, whereas low values of recharge may allow for accumulation of PFAS over time, resulting in a groundwater detection. Alternatively, low values of recharge may indicate that PFAS detections occur where natural recharge has been supplemented by imported sources of surface water or by agricultural irrigation water. For example, in areas of the California Coastal Basins with low natural recharge, there are high rates of PFAS detections in groundwater. The California Coastal Basins include places such as Los Angeles, where natural recharge has been supplemented by imported sources of recharge for decades.

The percent clay in soil had variable model influence that can best be observed in partial dependence plots (fig. S14). At very low values of clay content (<~10%), SHAP values were generally positive, whereas at mid-levels of clay content (~10 to ~35%), SHAP values were generally negative, suggesting that higher soil clay contents may impede PFAS transport to the groundwater through low hydraulic conductivity and/or enhanced sorption and retention (*47*, *48*). High percentages of clay (>~35%) generally resulted in positive SHAP values. Investigation into these high values indicated that several either resided in highly urbanized areas or were in agriculturally dominated areas where it is possible that biosolids from wastewater treatment plants (a well-known source of PFAS) or other amendments were added to improve clay-rich soil quality or that farmers have installed tile drainage or similar water management practices to improve drainage (*49*). Fracturing of the clay within the soil zone as a result of the high clay content may also increase preferential flow pathways for PFAS to be transported to groundwater more effectively. Back diffusion of PFAS from clay layers may also play a role, particularly in cases in which the system was loaded with PFAS, such as through biosolids spreading. It is also possible that clay and other variables are proxies for variables not included in the model that may contribute to complicated

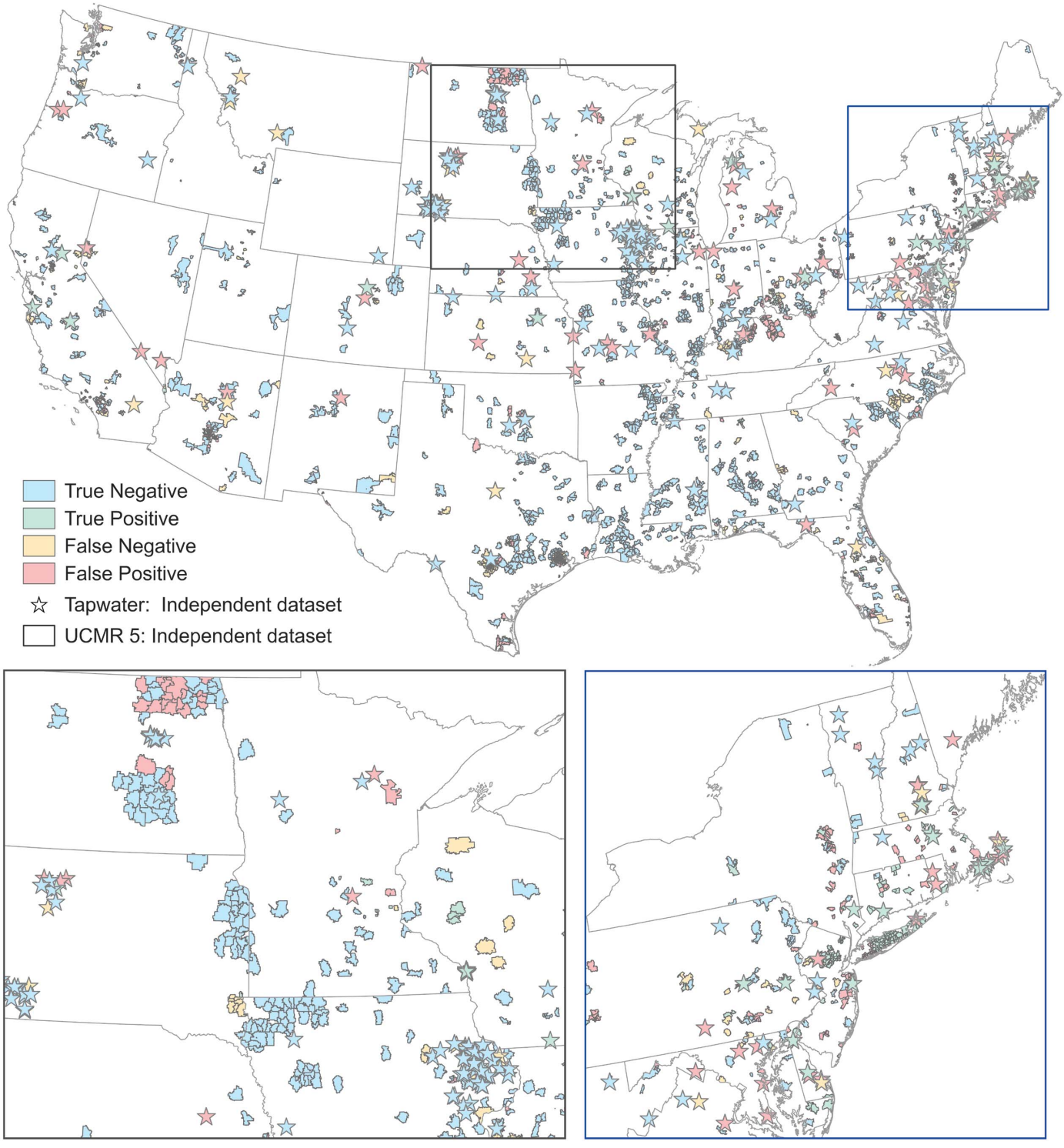

Fig. 4. Model validation for detection of PFAS with national independent datasets. Independent datasets for public water supply (UCMR 5) (*37*) and domestic supply (tapwater) (*8*) were evaluated against model results. The model probability threshold for detection of PFAS was set to 0.315. ZIP codes were classified as a predicted detection if >50% of the grid cells within each ZIP code exceeded the model probability threshold.

relationships. For example, clay could be a proxy for lithology or other climatic or geologic conditions. The model is inherently limited by datasets that have national coverage to allow for prediction, but could benefit from such data as it becomes available. Additional mechanistic studies on the role of clay in PFAS transport to groundwater over a range of climatic conditions would also be beneficial in deciphering relationships.

We observed more straightforward trends for nitrogen from septic systems, with low values of nitrogen loading from septic systems associated with negative SHAP values and high values of nitrogen loading associated with

positive SHAP values. Septic systems are known to be sources of PFAS to groundwater (*50*), which aligns with model results.

Last, short distances to the nearest site potentially handling, using, and/or releasing PFAS resulted in positive SHAP values, whereas greater distances resulted in primarily negative SHAP values. This aligns with previous modeling efforts in which proximity to PFAS sources was correlated with PFAS occurrence (*7*, *8*).

SHAP values for every predictor variable and every grid cell across the conterminous United States are provided in fig. S15, which depicts how different variables are important in different areas of the country. For example, urban land use, clay, and nitrogen from septic systems generally have positive SHAP values in Connecticut, whereas these SHAP values are largely negative in places such as Nevada.

Comparison of model to independent test data

We performed 10-fold model cross-validation tuning as part of the model building. In addition, we performed model validation using several completely independent test datasets, including data from UCMR 5; a national domestic well dataset from USGS; and both domestic and public supply data from Wisconsin, a state with limited training data available. Overall, model accuracies were consistent regardless of the groundwater depth to drinking water supplies. In other words, areas of the conterminous United States with shallower depths to drinking water supplies were modeled as well as areas of the country with deeper depths to drinking water supplies (figs. S10 and S16). We calculated observed and modeled detection frequencies for each threshold and for each dataset (Table 1). Modeled detection frequencies at the 0.5 threshold were typically similar to observed detection frequencies, whereas the 0.315 threshold typically overestimated detection frequency. Therefore, the 0.315 threshold should be seen as an upper-limit estimate that may overestimate occurrence but may cover areas with PFAS contamination that would otherwise be missed if using a 0.5 threshold. Point comparisons enabled accuracy, sensitivity, and specificity metrics as well (Table 1). Typically, accuracy and specificity increased and sensitivity decreased when shifting the threshold from 0.315 to 0.5 (Table 1). This model provides flexibility to water resource managers and homeowners because the threshold can be changed to fit the needs of the users. For example, although a lower threshold may overestimate detection frequency, it results in higher sensitivity and provides more certainty that areas that may have PFAS are not overlooked when designing sampling plans.

UCMR 5

In July 2023, the UCMR 5 program published the first batch of public water system data for PFAS and lithium (*37*, *51*), providing an opportunity to use independent public supply data to evaluate our model performance. These data were not available at the time of model development and are not suitable for the model because groundwater depths are unknown and exact source water locations are not disclosed. Further, these results are at the entry point to the distribution system and may or may not have undergone treatment, whereas the model predicts raw groundwater occurrence. Because our model output had finer resolution than that of the ZIP code–level UCMR 5 data, the 50th percentile was evaluated to classify the ZIP code as either a detect or nondetect on the basis of the gridded model results (50% of the cells within the ZIP codes reporting UCMR 5 results were required to be predicted as a detection to count the ZIP code block as a detection). Additional percentile cutoffs were evaluated and can be found in fig. S17. The model output was well aligned with the UCMR 5 data, with accuracy between 0.64 and 0.67 for model thresholds of 0.315 and 0.5, respectively (Table 1 and table S9). We also evaluated model performance by binning states that did and did not have model training data available. Similar performance was found in states that did not have model training data available compared with states that did have model training data available (Table 1). This is likely because the training data input covered a broad range of land use, geologic, and hydrologic settings (figs. S5 and S6), allowing the model to extrapolate well to unsampled locations.

USGS domestic tapwater

To validate the domestic water supply predictions, we conducted a separate validation test using domestic tapwater data (n = 255 wells) collected by the USGS from wells before any treatment (*8*). Results for a 0.5 threshold produced higher accuracy and specificity than a threshold of 0.315 (Table 1 and table S10). The model performed reasonably well, despite uncertainties such as unknown domestic well depths in the tapwater dataset and dataset differences, including the number of compounds analyzed (Fig. 4). Binning results by states with and without model training data indicated higher overall accuracy and specificity for states without training data. Although sensitivity was lower in states without model training data available, this may not be reflective of true sensitivity because there were only 16 data points in this category. Overall, the metrics indicate that the model performed well across the conterminous United States for domestic water supply predictions.

Wisconsin domestic well water and public supply

Last, we also evaluated model performance in the state of Wisconsin to better understand whether the model may be useful on a statewide level. Wisconsin had limited training data available (10 samples) and is therefore a useful state to evaluate.

We gathered previously published data on untreated domestic well water (*52*). Overall, model accuracy for a threshold of 0.315 (0.63, n = 448 wells) was similar to UCMR 5 and the national domestic tapwater datasets, although sensitivity (0.34) was lower, and specificity (0.78) was higher, indicating that the model may underpredict PFAS occurrence (Table 1 and table S11). However, the model and this dataset are not directly comparable because the Wisonsin domestic well dataset only targeted wells that were <40 feet below the static water level (*52*). Because model predictions are made at a certain depth (fig. S10) and specific depth to water for each grid cell, the data were processed to be more directly comparable by limiting the domestic samples to only those that fell in grid cells <40 feet below the water level. For example, each model grid cell predicts the probability of PFAS detection at a specific groundwater depth. It is only appropriate to compare observed (validation) data to the grid cell on which the point falls in cases in which the model well depth is also only <40 feet below the water level. Otherwise, model predictions are for deeper depths that do not match the available domestic validation dataset from Wisconsin. To calculate where model depths were <40 feet below the water table, depth to water was subtracted from the model depth (fig. S18). Once the datasets were comparable, accuracy rose to 0.70 (n = 40 wells), and sensitivity and specificity increased to 0.43 and 0.85, respectively (Table 1). A threshold of 0.5 at the appropriate water depths increased performance of accuracy and specificity (accuracy, 0.75; sensitivity, 0.36; specificity, 0.96). This suggests that model performance would improve if well depths were known for the other validation data (UCMR 5 and domestic tapwater) and directly paired with model depths.

For public supply in Wisconsin (*53*), data were censored to the common MDL of our dataset, systems reliant on surface water were removed, and a system was considered to contain PFAS if there were PFAS detections in any samples within that supply for any sample point (table S12). Samples may or may not have gone through drinking water treatment, similar to UCMR 5 data. Similar trends were found from public water supply data gathered for the state of Wisconsin (table S12) compared with UCMR 5 results. Results (accuracy, 0.64; sensitivity, 0.64; specificity, 0.63) indicate a balance between sensitivity and specificity at a threshold of 0.315 (Table 1 and table S13). A threshold of 0.5 produced higher overall accuracy and specificy at the expense of sensitivity (accuracy, 0.74; sensitivity, 0.42; specificity, 0.81). It was also feasible to evaluate the estimated values of equivalent population predicted to

be affected for public supply for Wisconsin because the dataset contains information on population served by each public water supply. The data indicate that 1.3 million people are affected, or 49% of the public water systems tested. This matches the 1.3 million our model predicts (57% of the population using public supply from groundwater) at the 0.315 threshold (table S6), indicating excellent alignment between model predictions and data.

Independent validation synthesis

The public and domestic water results demonstrate how model predictions can effectively be used by adjusting probability thresholds to address priorities. To achieve the best accuracy, a threshold of 0.5 should be chosen. However, if a sampling plan is being developed and the goal is not to overlook any areas that may have PFAS in groundwater, a lower threshold of 0.315 would be advantageous. Lower or higher thresholds may also be chosen to boost sensitvitiy or specificity, respectively, depending on the end user's objectives.

Conclusions

This national predictive model provides information to states, resource managers, and domestic well owners and can be used to help guide sampling toward areas where exposure to PFAS could be an issue. The results are available for public consumption (*17*), which allows users to evaluate results in their region. Users should not overinterpret specific grid cell(s) a house may fall on but should rather evaluate larger-scale regional and national trends. Users can use the probabilities with or without applying a threshold to better understand predicted groundwater quality in their area. If users do apply a threshold, they should keep in mind that the 0.315 threshold may overestimate occurrence but is more likely to capture areas with PFAS contamination that may otherwise be overlooked. Model predictions are for the source groundwater, before any treatment. The footprint of PFAS occurrence at the depth of public and domestic water supply may continue to expand as groundwater is recharged to aquifers and migrates downward over time, given the extensive PFAS contamination reported in air, rain, and soil, among many other sources. Awareness and regular monitoring of PFAS coupled with appropriate drinking water treatment will help reduce human exposure from drinking water sources.

REFERENCES AND NOTES

1. I. T. Cousins, J. H. Johansson, M. E. Salter, B. Sha, M. Scheringer, *Environ. Sci. Technol.* **56**, 11172–11179 (2022).
2. S. E. Fenton *et al*., *Environ. Toxicol. Chem.* **40**, 606–630 (2021).
3. E. M. Sunderland *et al*., *J. Expo. Sci. Environ. Epidemiol.* **29**, 131–147 (2019).
4. G. T. Ankley *et al*., *Environ. Toxicol. Chem.* **40**, 564–605 (2021).
5. G. B. Post, *Environ. Toxicol. Chem.* **40**, 550–563 (2021).
6. EPA, "Per- and Polyfluoroalkyl Substances National Primary Drinking Water Regulation," 40 Code of Federal Regulations (CFR) § 141 and 142 (2024).
7. P. B. McMahon *et al*., *Environ. Sci. Technol.* **56**, 2279–2288 (2022).
8. K. L. Smalling *et al*., *Environ. Int.* **178**, 108033 (2023).
9. EPA, "The Fifth Unregulated Contaminant Monitoring Rule (UCMR 5) program overview fact sheet," EPA 815-F-21-009 (EPA, 2021).
10. EPA, "National characteristics of drinking water systems serving 10,000 or fewer people," EPA 816-R-10-022 (EPA, 2011).
11. C. A. Dieter *et al*., *Estimated use of water in the United States in 2015*, vol. 1441, US Geological Survey Circular (USGS, 2018).
12. X. C. Hu, B. Ge, B. J. Ruyle, J. Sun, E. M. Sunderland, *Environ. Sci. Technol. Lett.* **8**, 596–602 (2021).
13. S. George, A. Dixit, *J. Environ. Manage.* **295**, 113359 (2021).
14. N. Fernandez, A. P. Nejadhashemi, C. Loveall, *Water Res.* **243**, 120307 (2023).
15. J. Dong, G. Tsai, C. I. Olivares, *ACS ES T Water* **4**, 969–981 (2023).
16. X. C. Hu, M. Dai, J. M. Sun, E. M. Sunderland, *Curr. Environ. Health Rep.* **10**, 45–60 (2023).
17. A. K. Tokranov *et al*., Predictions of PFAS occurrence in groundwater at the depth of drinking water supplies in the conterminous United States: Data and model archive, USGS data release (2024); https://doi.org/10.5066/P93RXTKJ.
18. T. Chen *et al*., xgboost: Extreme Gradient Boosting, R package version 1.7.5.1 (2023); https://CRAN.R-project.org/package=xgboost.
19. T. D. Johnson, K. Belitz, L. J. Kauffman, E. Watson, J. T. Wilson, *Sci. Total Environ.* **806**, 150618 (2022).
20. T. D. Johnson, K. Belitz, M. A. Lombard, *Sci. Total Environ.* **687**, 1261–1273 (2019).
21. J. C. Scott, "Computerized stratified random site-selection approaches for design of a ground-water-quality sampling network," vol. 90-4101, US Geological Survey Water-Resources Investigations Report (USGS, 1990).
22. K. Belitz *et al*., *ACS ES T Water* **2**, 2645–2656 (2022).
23. K. Belitz, M. S. Fram, T. D. Johnson, *Environ. Sci. Technol.* **49**, 8330–8338 (2015).
24. B. C. Jurgens, M. Jasper, D. H. Nguyen, G. L. Bennett, USGS California Groundwater Ambient Monitoring and Assessment Program Priority Basin Project (GAMA-PBP) groundwater-quality results—Assessment and trends (USGS, 2018); https://doi.org/10.5066/P91WJ2G1.
25. US Geological Survey Upper Midwest Water Science Center, Principal aquifers of the 48 conterminous United States, Hawaii, Puerto Rico, and the U.S. Virgin Islands, USGS data release (2003); https://doi.org/10.5066/P9Y2HOUJ.
26. B. D. Lindsey, B. J. Fleming, P. J. Goodling, A. M. Dondero, *J. Hydrol.* **627**, 130427 (2023).
27. Materials and methods are available as supplementary materials.
28. A. E. LaMotte, Estimated nitrogen from septic for the conterminous United States, 2010 (SepN_CONUS_bg_2010), USGS data release (2018); https://doi.org/10.5066/P9QTGSI7.
29. J. Elith, J. R. Leathwick, T. Hastie, *J. Anim. Ecol.* **77**, 802–813 (2008).
30. K. M. Ransom, B. T. Nolan, P. E. Stackelberg, K. Belitz, M. S. Fram, *Sci. Total Environ.* **807**, 151065 (2022).
31. L. A. DeSimone, J. P. Pope, K. M. Ransom, *J. Hydrol. Reg. Stud.* **30**, 100697 (2020).
32. P. Grandjean, E. Budtz-Jørgensen, *Environ. Health* **12**, 35 (2013).
33. B. C. Jurgens *et al*., *Commun. Earth Environ.* **3**, 153 (2022).
34. M. L. Erickson *et al*., *Environ. Sci. Technol.* **55**, 5791–5805 (2021).
35. D. W. Hosmer, S. Lemeshow, *Applied Logistic Regression* (Wiley, ed. 2, 2000).
36. L. J. Kauffman, J. R. Degnan, K. Belitz, P. E. Stackelberg, M. L. Erickson, Data for depth of groundwater used for drinking-water supplies in the United States, USGS data release (2021); https://doi.org/10.5066/P94640EM.
37. US Environmental Protection Agency, "The Fifth Unregulated Contaminant Monitoring Rule (UCMR 5) data summary: July 2023," EPA 815-S-23-003 (EPA, 2023).
38. A. Cordner *et al*., *Environ. Sci. Technol.* **55**, 9630–9633 (2021).
39. K. M. C. Malecki, A. A. Schultz, D. J. Severtson, H. A. Anderson, J. A. VanDerslice, *Sci. Total Environ.* **601-602**, 1533–1543 (2017).
40. R. Mulhern, B. Grubbs, K. Gray, J. MacDonald Gibson, *Sci. Total Environ.* **806**, 150448 (2022).
41. S. M. Lundberg, S.-I. Lee, A unified approach to interpreting model predictions. arXiv:1705.07874 [cs.AI] (2017).
42. D. Salvatore *et al*., *Environ. Sci. Technol. Lett.* **9**, 983–990 (2022).
43. D. Ma, H. Zhong, J. Lv, Y. Wang, G. Jiang, *J. Environ. Sci)* **112**, 71–81 (2022).
44. M. Sörengård, J. Kikuchi, K. Wiberg, A. Lutz, *Chemosphere* **295**, 133944 (2022).
45. W. Zhu *et al*., *J. Hazard. Mater.* **438**, 129479 (2022).
46. P. B. McMahon, N. Plummer, J. K. Böhlke, S. D. Shapiro, S. R. Hinkle, *Hydrogeol. J.* **19**, 779–800 (2011).
47. F. Xiao, X. Zhang, L. Penn, J. S. Gulliver, M. F. Simcik, *Environ. Sci. Technol.* **45**, 10028–10035 (2011).
48. C. E. Schaefer, D. Drennan, A. Nickerson, A. Maizel, C. P. Higgins, *J. Contam. Hydrol.* **241**, 103814 (2021).
49. M. L. Macrae *et al*., *J. Environ. Qual.* **48**, 1347–1355 (2019).
50. L. A. Schaider, J. M. Ackerman, R. A. Rudel, *Sci. Total Environ.* **547**, 470–481 (2016).
51. EPA, *Occurrence data from the Unregulated Contaminant Monitoring Rule* (2023); https://www.epa.gov/dwucmr/occurrence-data-unregulated-contaminant-monitoring-rule.
52. M. Silver *et al*., *Environ. Sci. Technol.* **57**, 17415–17426 (2023).
53. Wisconsin Department of Natural Resources, Wisconsin Drinking Water System Portal (Wisconsin Department of Natural Resources,2024); https://apps.dnr.wi.gov/dwsportalpub.

ACKNOWLEDGMENTS

We thank E. Woodward and M. Lombard for their thoughtful reviews that improved this paper and K. Belitz for his feedback on model performance metrics. We thank J. Flashinski, A. DeWeese, J. Schutz, and A. Ihlenfeldt from the Wisconsin Department of Natural Resources and M. Silver for their willingness to share public and domestic supply data in Wisconsin. Last, we thank the anonymous journal reviewers for their valuable comments and suggestions that strengthened this manuscript. Any use of trade, firm, or product names is for descriptive purposes only and does not imply endorsement by the US government. **Funding:** This work was supported by the USGS National Water Quality Program; USGS Ecosystems Mission Area Environmental Health Program; and California State Water Resources Control Board Groundwater Ambient Monitoring and Assessment Program agreement 20-013-250-1. **Author contributions:** Conceptualization: A.K.T., B.D.L., and M.S.F. Data curation: A.K.T., L.M.B., B.D.L., M.S.F., E.W., D.I.D., S.A.V., J.A.K., B.C.J., K.L.S., and P.M.B. Formal analysis: A.K.T. and K.M.R. Methodology: A.K.T., K.M.R., B.D.L., P.E.S., and M.S.F. Investigation: A.K.T., K.M.R., B.D.L., L.M.B., E.W., D.I.D., M.S.F., S.A.V., J.A.K., and B.C.J. Visualization: A.K.T. and K.M.R. Validation: A.K.T., K.L.S., and P.M.B. Funding acquisition: A.K.T., B.D.L., and M.S.F. Project administration: B.D.L. Supervision: A.K.T., B.D.L., and M.S.F. Writing – original draft: A.K.T. Writing – review and editing: A.K.T., K.M.R., L.M.B., B.D.L., E.W., D.I.D., P.E.S., M.S.F., S.A.V., J.A.K., B.C.J., K.L.S., and P.M.B. **Competing interests:** The authors declare that they have no competing interests. **Data and materials availability:** All data, model object, code, and model input and output files are publicly available as a USGS data release, DOI 10.5066/P93RXTKJ (*17*). Data used as independent model validation are cited in the main reference list (*8*, *37*, *51–53*).

SUPPLEMENTARY MATERIALS

science.org/doi/10.1126/science.ado6638
Materials and Methods
Supplementary Text
Figs. S1 to S18
Tables S1 to S13
References (*54–84*)

Submitted 16 February 2024; resubmitted 31 May 2024
Accepted 10 October 2024
Published online 24 October 2024
10.1126/science.ado6638

Predictions of groundwater PFAS occurrence at drinking water supply depths in the United States

Andrea K. Tokranov, Katherine M. Ransom, Laura M. Bexfield, Bruce D. Lindsey, Elise Watson, Danielle I. Dupuy, Paul E. Stackelberg, Miranda S. Fram, Stefan A. Voss, James A. Kingsbury, Bryant C. Jurgens, Kelly L. Smalling, and Paul M. Bradley

Science **386** (6723), . DOI: 10.1126/science.ado6638

Editor's summary

Forever chemicals such as per- and polyfluoroalkyl substances (PFAS) are potential hazards for the environment and human health. The detection of PFAS in groundwater is particularly concerning, especially for drinking water sources. Tokranov *et al*. compiled a large database of US groundwater observations as the basis for a model to estimate the probability of PFAS contamination based on well depth. The data come from a range of well types, including those for observation, domestic tap water, and public water supply. The model highlights that about 80 million people in the conterminous US rely on groundwater with detectable amounts of PFAS before treatment. —Brent Grocholski